



**HAL**  
open science

## Laser-assisted evaporative cooling of anions

G Cerchiari, P Yzombard, A Kellerbauer

► **To cite this version:**

G Cerchiari, P Yzombard, A Kellerbauer. Laser-assisted evaporative cooling of anions. *Physical Review Letters*, 2020. hal-03000318

**HAL Id: hal-03000318**

**<https://hal.science/hal-03000318>**

Submitted on 11 Nov 2020

**HAL** is a multi-disciplinary open access archive for the deposit and dissemination of scientific research documents, whether they are published or not. The documents may come from teaching and research institutions in France or abroad, or from public or private research centers.

L'archive ouverte pluridisciplinaire **HAL**, est destinée au dépôt et à la diffusion de documents scientifiques de niveau recherche, publiés ou non, émanant des établissements d'enseignement et de recherche français ou étrangers, des laboratoires publics ou privés.

# Laser-assisted evaporative cooling of anions

G. Cerchiari, P. Yzombard, and A. Kellerbauer\*

Max Planck Institute for Nuclear Physics, Saupfercheckweg 1, 69117 Heidelberg, Germany

(Dated: May 12, 2020)

We report the first cooling of atomic anions by laser radiation.  $O^-$  ions confined in a linear Paul trap were cooled by selectively photodetaching the hottest particles. For this purpose, anions with the highest total energy were illuminated with a 532 nm laser at their maximal radial excursion. Using laser–particle interaction, we realized a both colder and denser ion cloud, achieving a more than threefold temperature reduction from 1.15 eV to 0.33 eV. Compared with the interaction with a dilute buffer gas, the energy-selective addressing and removal of anions resulted in lower final temperatures, yet acted 10 times faster and preserved twice as large a fraction of ions in the final state. An ensemble of cold negative ions affords the ability to sympathetically cool any other negative ions species, enabling or facilitating a broad range of fundamental studies from interstellar chemistry to antimatter gravity. The technique can be extended to any negative ion species that can be neutralized via photodetachment.

Laser cooling, which reduces the kinetic energy of neutral or charged particles, is one of the most important experimental tools in atomic physics. It allows the cooling of particle beams or ensembles to temperatures below that of the surrounding apparatus, well below 1 K. Ultracold temperatures are a prerequisite for many groundbreaking applications, such as ultra-precise clocks [1], quantum information [2], quantum computation [3], or the study of matter waves with Bose–Einstein condensates [4, 5]. In the case of charged particles, laser cooling enables the formation of Coulomb crystals, regularly ordered structures that form when the electrostatic interaction prevails over thermal motion [6]. One interesting application of laser-cooled ultracold ions is the sympathetic cooling of another particle species. For instance, highly charged  $^{40}\text{Ar}^{13+}$  ions have been cooled into an ordered crystalline structure suitable for precision spectroscopy by interacting with  $\text{Be}^+$  ions at mK temperatures [7]. Other state-of-the-art experiments have combined trapped ions with a magneto-optical trap in such a way that the laser-cooled neutral atoms constitute a buffer medium which cools the trapped ions by collisions [8, 9].

In negative ions, the electronic binding is characterized by a short-range potential instead of the infinite-range Coulomb potential. Because of their fragile nature, the laser cooling of negative ions has not yet been achieved. Laser-cooled anions would open the field of ultra-precision studies to a new kind of system. Furthermore, they could be used to sympathetically cool any other negatively charged particles [10]. In the case of antimatter, a neutral buffer medium cannot be used for cooling due to the risk of annihilation, whereas the repelling electric charge of anions would prevent them from annihilating with antiprotons. In this way, a sample of ultracold antiprotons could be prepared by collisions with laser-cooled negative ions. Antihydrogen subsequently formed with these antiprotons would have almost the same low temperature due to the large mass ratio of antiproton to positron. This antihydrogen production technique would open the way for a variety of high-precision antimatter experiments. For instance, a beam of antihydrogen at  $\approx 100$  mK is a prerequisite for an antimatter gravity measurement to test the weak equivalence principle

using a moiré deflectometer [11].

Due to the weak binding of the valence electron, only very few atomic [12, 13] or molecular [14, 15] anions are amenable to laser cooling. Recently,  $\text{La}^-$  has been identified as the most promising atomic-anion candidate to date [16, 17]. The potential Doppler cooling transition has been fully characterized [18, 19]. The existence of a dark state, as well as photodetachment of the excited  $\text{La}^-$  by the cooling laser, impose an upper limit of 100 K on the initial temperature. Starting from that temperature, an ensemble of  $\text{La}^-$  ions could be cooled to the Doppler temperature  $T_D = 0.17 \mu\text{K}$  within a few seconds. When ions are loaded into an ion trap, they typically have temperatures of several ten thousand K. In order to precool them to the starting temperature for Doppler cooling, we have implemented a scheme based on the selective laser photodetachment of the hottest trapped particles, as suggested almost thirty years ago [20]. This technique is a variant of evaporative cooling, which is a well-established cooling mechanism for atoms [21] and, to a lesser extent, ions [22]. Evaporative cooling by photodetachment is only applicable to (atomic or molecular) *anions*, because neither cations nor negative subatomic particles can be removed from an ion trap by photodetachment. In this Letter we report the successful cooling of  $O^-$  ions with this technique, employing geometrical selection. This is the first demonstration of the direct cooling of a negative ion species using optical radiation.

The experiments reported here were carried out with  $O^-$  ions (electron affinity  $E_A = 1.4611136(9)$  eV [23], using the most recent conversion factor from  $\text{m}^{-1}$  to eV [24]) confined in a linear Paul trap. The trap, the trapping method, as well as the detection technique are described in detail in Ref. [25]. Briefly, the linear trap is composed of four cylindrical parallel electrodes (rods). A cross-sectional view is shown in Fig. 1. The rods have a diameter of 14.8 mm and a distance between the trap axis and the inner electrode surface of  $r_0 = 7$  mm. A radiofrequency (RF) signal is applied to one pair of opposing rods, whereas the signal on the second pair of rods has a phase shift of  $\pi$ . The applied RF has a frequency of  $\Omega_{RF}/(2\pi) = 1.938$  MHz and an amplitude (peak-to-peak) of  $V_{pp} = 225(20)$  V. The amplitude was chosen for optimal ion

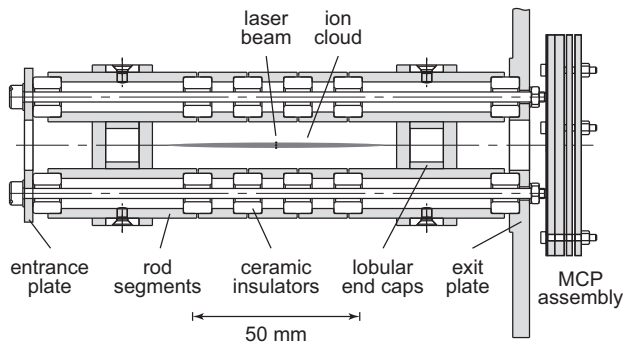


FIG. 1. Schematic drawing of the linear Paul trap. Ions enter the trap from the left and exit towards the MCP detector to the right.

loading. Additional electrodes (lobe-shaped end caps) provide axial ion confinement in a region of 65(5) mm length. Photodetachment of the anions is achieved by the light of a 532 nm laser ( $h\nu = 2.33$  eV) focused on the trap region.

The trap is loaded by allowing an ion beam with current  $\approx 800$  pA to pass through the trap for 100 s while the longitudinal trap potentials are in loading configuration. After the loading phase, the trap is closed by raising the potential of the downstream end cap and the system is left to evolve for 10 s until it reaches equilibrium. This settling time agrees with typical thermalization rates of  $\approx 1$ –5 s encountered in ion–ion Coulomb collisions [26, 27]. In this way, reproducible initial conditions for the ensuing experiments are established. After the loading process,  $1.5$ – $2.0 \times 10^4$  anions with an average density of  $3$ – $5 \times 10^4$  cm $^{-3}$  are typically confined in the trap. The ion cloud is strongly elongated along the axis with a typical aspect ratio of 1:40. Most of the anions are O $^-$  and a small fraction ( $< 10\%$ ) is composed of contaminants. These particles with a mass of 28–39 u could not be clearly identified [25], but remain in the trap over very long times and are unaffected by the green laser light. These background ions are apparently less prone to recombination with residual gas due to their higher electron affinity.

The number  $N$  of trapped anions and their temperature  $k_B T$  are recorded destructively. At the end of each trial, the trap is opened by switching the downstream end cap to the rod potential. The trapped particles are then free to move towards a micro-channel plate (MCP) detector located at a distance of  $\approx 5$  mm from the exit plate of the trap. The MCP is equipped with a phosphor screen that converts the amplified current of secondary electrons into light, which in turn is recorded with a digital camera. The MCP image is an axial projection of the ejected ion cloud. The radially confining pseudopotential has approximately cylindrical symmetry near the axis, whereas for large excursions the radial potential becomes slightly asymmetrical. The axial confinement can be considered a simple box potential. Assuming thermal equilibrium, anions arrange in the trap according to the Boltzmann distribution. Furthermore, in the approximation of a harmonic radial potential, the average values of the kinetic and potential

energies are equal (equipartition) [20].

Thus, the radial temperature can be extracted by fitting the density function  $p(r) \propto \exp(-r^2/\sigma^2)$  to the radial intensity of the images. The spatial width  $\sigma$  of the anion cloud is related to the temperature of the ions by the expression  $\sigma = \sqrt{k_B T / (m\omega^2)}$ , where  $k_B$  is the Boltzmann constant and  $\omega$  is the angular frequency of the anions' radial oscillations in the trap. The latter can be approximated by  $\omega = \sqrt{2eV_{pp} / (2m\Omega_{RF}r_0^2)}$ , where  $m$  is the anion mass [28]. The systematic uncertainty of the radial position was estimated by a Monte Carlo simulation to be of the order of 10%. This uncertainty and that of  $V_{pp}$  affect all acquisitions similarly. Therefore, these systematic uncertainties are omitted in all graphs. The axial ejection was not locked to the RF phase, and no dependence of the measured ion temperature on this (arbitrary) phase was observed.

The laser beam with a Gaussian radial profile is focused into the trap region using a biconvex lens with focal length 300 mm located 294(1) mm from the focus. The position of the laser beam inside the trap is adjusted by displacing the lens in the plane perpendicular to the light propagation. In a Cartesian reference frame  $(x, y, z)$ , where the trap is aligned with the  $z$  axis and the laser light propagates in the  $y$  direction, the expression for the laser beam intensity  $I$  as a function of the  $x$  coordinate is thus

$$I(x) = \frac{I_0}{\sqrt{\pi}w} \exp\left(-\frac{(x-d)^2 + z^2}{w^2}\right), \quad (1)$$

where  $w = 0.35(25)$  mm is the diameter of the beam waist and  $d$  is the displacement of the laser beam in the  $x$  direction.

The pressure in the experiment chamber is about  $5 \times 10^{-10}$  mbar. Due to collisions of anions with residual gas we observe both a buffer-gas cooling effect with a final temperature  $k_B T \approx 0.75$  eV and a limited lifetime ( $< 2$  min). In order to achieve more efficient cooling, the most energetic anions should be removed from the trap. Those particles with the highest total energy are also those with the highest radial amplitude at their maximal radial excursion. By adjusting the displacement  $d$  of the laser beam waist from the axis, it is possible to heat or cool the ion ensemble by selectively interacting with anions orbiting close to or far from the trap axis. If  $d^*$  denotes the laser displacement for which neither a net cooling nor a net heating effect is achieved, setting the average energy of the illuminated anions equal to the total average energy per anion in the trap we obtain the expression  $d^* = \sqrt{(w^2 + \sigma^2)}/2$ , which will be used to support the interpretation of our experimental results.

We performed three sets of measurements to demonstrate cooling by selective photodetachment. In all cases, the ion evolution with and without the laser radiation interacting with the anions was recorded for the same time duration. In this way, it was possible to directly compare the evolution of the system with and without laser interaction.

We first varied the displacement  $d$  of the laser beam from the trap axis by adjusting the position of the focusing lens.

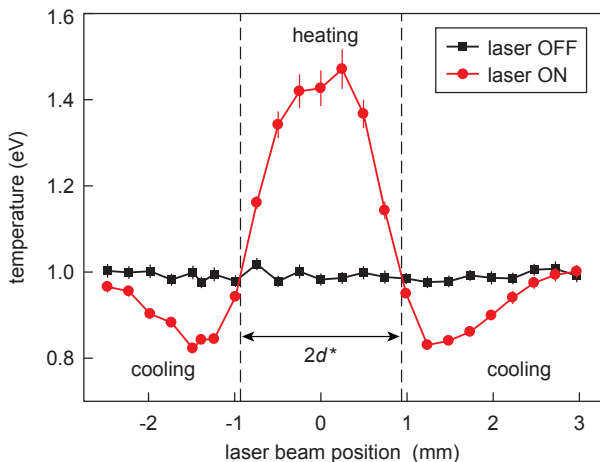


FIG. 2. Final anion temperature as a function of the lens (and hence laser beam) displacement from the trap axis after 12 s of laser illumination. Vertical dashed lines indicate the lens positions at which neither ion heating nor cooling occurs.

178 The laser shutter was opened for 12 s at a laser power of  
 179 11 mW. Figure 2 shows a comparison of the final tempera-  
 180 res obtained with and without illumination. A tempera-  
 181 ture reduction is observed if ions with large oscillation amplitudes  
 182 are photodetached, while the ensemble is *heated* if ions closer  
 183 to the trap axis are removed. The laser beam displacement  $d^*$ ,  
 184 the position where neither cooling nor heating occurs, corre-  
 185 sponds to the cross-over points of the two data sets shown  
 186 in the figure. The value  $d_{\text{exp}}^* = 0.93(5)$  mm compares well  
 187 with the calculated value  $d_{\text{theo}}^* = 1.10(15)$  mm, thus support-  
 188 ing the explanation of the cooling mechanism.

190 We then positioned the laser beam to remove anions at a  
 191 distance  $d = 1.5$  mm from the trap axis (minima of the red line  
 192 in Fig. 2, maximum cooling) and measured the storage time as  
 193 a function of the laser power from 6 mW to 27 mW. Figure 3  
 194 shows that, as expected, the lifetime of the anions decreases  
 195 due to photodetachment. The decrease in the number of ions  
 196 was modeled with an exponential decay law with a constant  
 197 fraction  $N_{\text{cont}} = 1.3 \times 10^3$  to account for contaminant ions that  
 198 resist photodetachment:

$$N = N_0 \exp\left(-\frac{t}{\tau}\right) + N_{\text{cont}}. \quad (2)$$

200 The fit results of the ion lifetimes are indicated in Tab. I.

202 As mentioned above, the ion temperature of the trapped an-  
 203 ions decreases even without laser irradiation, due to cooling  
 204 by collisions and thermalization with residual gas. However,  
 205 Fig. 4 shows that the cooling rate is strongly enhanced by the  
 206 detachment laser. The thermalization curve was fitted with the  
 208 following expression:

$$T = (T_0 - T_{\infty}) \exp\left(-\frac{t}{\theta}\right) + T_{\infty}, \quad (3)$$

209 where  $T_0$  is the starting temperature,  $T_{\infty}$  is the asymptotic final  
 210 temperature, and  $\theta$  is the characteristic cooling time. The pa-  
 211 rameters obtained from the fits are given in Tab. II. The cool-

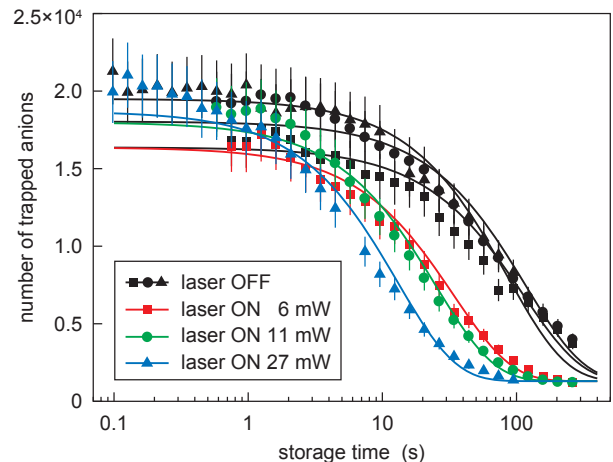


FIG. 3. Number of  $\text{O}^-$  ions in the trap as a function of storage time. The measurements with the laser on were acquired with the laser beam positioned at  $d = 1.5$  mm (Eq. 1). Data sets with laser on and off denoted with the same symbols were taken contemporaneously under otherwise identical conditions. Solid lines are fits to the data using the function of Eq. 2

TABLE I. Lifetime parameters extracted using Eq. 2 with and without laser illumination. Grouped data sets were taken under similar conditions.

Laser power	$N_0 \times 10^{-4}$	$\tau$ (s)
OFF	1.51(5)	113(7)
6mW	1.51(4)	34(1)
OFF	1.67(4)	117(6)
11 mW	1.67(4)	25.1(9)
OFF	1.82(2)	86(4)
27 mW	1.74(5)	13.0(6)

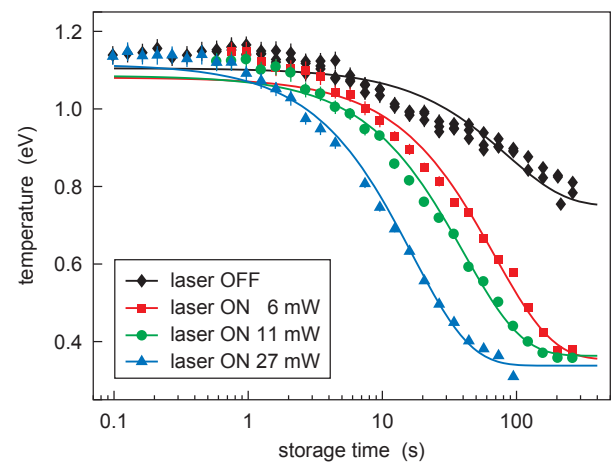


FIG. 4. Temperature of  $\text{O}^-$  anions in the trap as a function of storage time. The measurements with the laser were acquired with  $d = 1.5$  mm (Eq. 1). Solid lines are fits to the data using the function of Eq. 3.

TABLE II. Starting temperature, asymptotic final temperature and cooling time obtained from the fit of Eq. 2 to the data of Fig. 4.

Laser power	$T_0$ (eV)	$T_\infty$ (eV)	$\theta$ (s)
OFF	1.105(7)	0.75 <sup>a</sup>	85(5)
6 mW	1.08(2)	0.35(1)	69(4)
11 mW	1.09(1)	0.363(7)	40(2)
27 mW	1.12(2)	0.338(7)	16.8(7)

<sup>a</sup> Parameter obtained from fit of Fig. 5 and held fixed for this fit

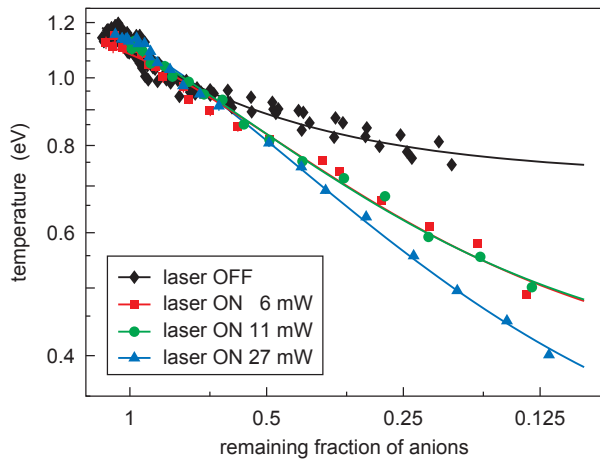


FIG. 5. Anion temperature as a function of the fraction of ions remaining in the trap. The number of remaining anions is normalized to the initial population before cooling. Error bars are comparable to the size of the data points. Solid lines are second-order polynomial fits and are meant to guide the eye.

212

213 ing rate  $\theta$  is enhanced in the presence of the laser light, and  
 214 more so for higher laser powers. Most importantly, the asymptotic  
 215 final temperature  $T_\infty$  is also significantly lower with the  
 216 laser on ( $\approx 0.35$  eV) than without laser ( $\approx 0.75$  eV).

217 Adopting this cooling scheme, it was possible to prepare a  
 218 larger ensemble of anions at a lower temperature than without  
 219 laser excitation. To highlight this effect, Fig. 5 shows the ion  
 220 temperature as a function of the fraction of anions remaining  
 221 in the trap after cooling. For instance, when 3/4 of the anions  
 222 have been removed or lost, a temperature of 0.56(17) eV  
 223 is obtained by cooling at 27 mW laser power, compared to  
 224 0.80(24) eV with the laser off. To reach this condition the  
 225 laser interacted with the ions for  $< 20$  s, whereas a similar ion  
 226 loss took more than 10 times longer without laser due to the  
 227 lower loss rate with only collisional detachment.

228 Finally, we monitored the temperature of the stored anions  
 229 after a brief laser-induced cooling cycle. The system was prepared  
 230 in a similar condition as previously, with the laser beam  
 231 position fixed at  $d = 1.5$  mm. After selective photodetachment  
 232 during 12 s at a laser power of 11 mW, the ion cloud  
 233 was allowed to evolve freely in the trap. The result is shown  
 234 in Fig. 6, where the ion temperature is plotted as a function of  
 235

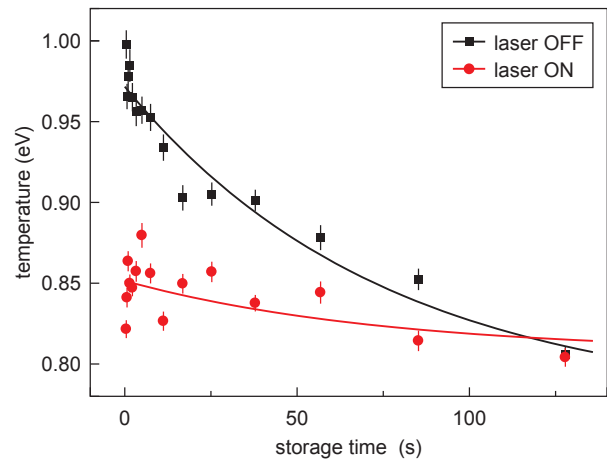


FIG. 6. Anion temperature as a function of storage time after the end of laser-induced cooling. Solid lines are simple exponential fits to the data.

238 the additional storage time after cooling. The figure shows that  
 239 the temperature reduction induced by the selective laser photo-  
 240 detachment persists quasi indefinitely. This indicates that after  
 241 evaporative cooling the entire anion cloud reaches thermal  
 242 equilibrium, as expected. While the data show that a similar  
 243 final temperature is also reached without selective photode-  
 244 tachment (at this low laser power), it is evident from Fig. 3  
 245 that the remaining fraction of ions is much smaller after 120 s  
 246 of storage time without laser ( $\approx 25\%$ ) than after 12 s of cool-  
 247 ing ( $\approx 75\%$ ).

247 In summary, we have presented the first cooling of trapped  
 248 negative ions induced by a light field. Laser light is used to  
 249 selectively remove the hottest particles by photodetachment.  
 250 The selection is applied by geometrically addressing those anions  
 251 with the largest radial oscillation amplitude. In this way, the ions'  
 252 temperature was reduced from 1.15 eV (13,000 K) to 0.33 eV  
 253 (3800 K) within about 100 s. With this technique the stored  
 254 anions can be cooled faster and to lower temperatures than can  
 255 be achieved by buffer gas cooling with residual gas. For instance,  
 256 we observed a more than twofold improvement in the limiting  
 257 final temperature, and that temperature can be reached about 10  
 258 times faster than by buffer gas cooling alone.

259 The technique can easily be extended to other negative ion  
 260 species, assuming a laser is available that can photodetach  
 261 them directly. State-of-the-art lasers for this task are generally  
 262 available, as typical electron affinities are of the order of  
 263 1 eV. Heavier anions up to  $^{139}\text{La}$  can be confined in our Paul  
 264 trap with an RF drive amplitude of 1.9–2.0 kV (peak-to-peak),  
 265 or at a correspondingly lower amplitude in a trap with smaller  
 266 radial dimensions. Faster cooling can be realized by illuminating  
 267 ions over a broader axial region and by compressing the ion  
 268 cloud in the axial direction to enhance overlap and ion-ion  
 269 collision rate. Displacing the laser position radially inward  
 270 during cooling could help optimize the cooling rate and decrease  
 271 ion losses. Finally, the cooling scheme could be

272 combined with an additional resonant excitation step, which  
 273 would allow the laser to be red-detuned for Doppler selection  
 274 of the hottest particles. This would enhance both the selectiv-  
 275 ity and the efficiency of the overall cooling process.

276 The authors thank the MPIK mechanical workshop for their  
 277 excellent work in constructing the linear RF trap. This work  
 278 was supported by the European Research Council (ERC) un-  
 279 der Grant No. 259209 (UNIC).

---

280 \* Corresponding author; a.kellerbauer@cern.ch

- 281 [1] J.-S. Chen, S. M. Brewer, C. W. Chou, D. J. Wineland, D. R.  
 282 Leibbrandt, and D. B. Hume, *Phys. Rev. Lett.* **118**, 053002  
 283 (2017).
- 284 [2] W. Rosenfeld, D. Burchardt, R. Garthoff, K. Redeker, N. Or-  
 285 tegel, M. Rau, and H. Weinfurter, *Phys. Rev. Lett.* **119**, 010402  
 286 (2017).
- 287 [3] N. Friis, O. Marty, C. Maier, C. Hempel, M. Holzäpfel, P. Ju-  
 288 rcevic, M. B. Plenio, M. Huber, C. Roos, R. Blatt, et al., *Phys.*  
 289 *Rev. X* **8**, 021012 (2018).
- 290 [4] M. H. Anderson, J. R. Ensher, M. R. Matthews, C. E. Wieman,  
 291 and E. A. Cornell, *Science* **269**, 198 (1995).
- 292 [5] K. B. Davis, M.-O. Mewes, M. R. Andrews, N. J. van Druten,  
 293 D. S. Durfee, D. M. Kurn, and W. Ketterle, *Phys. Rev. Lett.* **75**,  
 294 3969 (1995).
- 295 [6] M. Drewsen, *Physica B* **460**, 105 (2015).
- 296 [7] L. Schmöger, O. O. Versolato, M. Schwarz, M. Kohnen,  
 297 A. Windberger, B. Piest, S. Feuchtenbeiner, J. Pedregosa-  
 298 Gutierrez, T. Leopold, P. Micke, et al., *Science* **347**, 1233  
 299 (2015).
- 300 [8] W. G. Rellergert, S. T. Sullivan, S. J. Schowalter, S. Ko-  
 301 tochigova, K. Chen, and E. R. Hudson, *Nature* **495** (2013).
- 302 [9] B. Höltkemeier, P. Weckesser, H. López-Carrera, and M. Wei-  
 303 demüller, *Phys. Rev. Lett.* **116**, 233003 (2016).
- 304 [10] A. Kellerbauer and J. Walz, *New J. Phys.* **8**, 45 (2006).
- 305 [11] A. Kellerbauer et al. (AEGIS Proto-Collaboration), *Nucl. In-*  
 306 *strum. Methods B* **266**, 351 (2008).
- 307 [12] U. Warring, M. Amoretti, C. Canali, A. Fischer, R. Heyne, J. O.  
 308 Meier, C. Morhard, and A. Kellerbauer, *Phys. Rev. Lett.* **102**,  
 309 043001 (2009).
- 310 [13] C. W. Walter, N. D. Gibson, Y.-G. Li, D. J. Matyas, R. M. Alton,  
 311 S. E. Lou, R. L. Field, D. Hanstorp, L. Pan, and D. R. Beck,  
 312 *Phys. Rev. A* **84**, 032514 (2011).
- 313 [14] P. Yzombard, M. Hamamda, S. Gerber, M. Doser, and D. Com-  
 314 parat, *Phys. Rev. Lett.* **114**, 213001 (2015).
- 315 [15] S. Gerber, J. Fesel, M. Doser, and D. Comparat, *New J. Phys.*  
 316 **20**, 023024 (2018).
- 317 [16] S. M. O'Malley and D. R. Beck, *Phys. Rev. A* **81**, 032503  
 318 (2010).
- 319 [17] C. W. Walter, N. D. Gibson, D. J. Matyas, C. Crocker, K. A.  
 320 Dungan, B. R. Matola, and J. Rohlén, *Phys. Rev. Lett.* **113**,  
 321 063001 (2014).
- 322 [18] E. Jordan, G. Cerchiari, S. Fritzsche, and A. Kellerbauer, *Phys.*  
 323 *Rev. Lett.* **115**, 113001 (2015).
- 324 [19] G. Cerchiari, A. Kellerbauer, M. S. Safronova, U. I. Safronova,  
 325 and P. Yzombard, *Phys. Rev. Lett.* **120**, 133205 (2018).
- 326 [20] A. Crubellier, *J. Phys. B* **23**, 3585 (1990).
- 327 [21] W. Ketterle and N. J. Van Druten, *Adv. At. Mol. Opt. Phys.* **37**,  
 328 181 (1996).
- 329 [22] B. M. Penetrante, J. N. Bardsley, M. A. Levine, D. A. Knapp,  
 330 and R. E. Marrs, *Phys. Rev. A* **43**, 4873 (1991).
- 331 [23] W. Chaibi, R. J. Pelaez, C. Blondel, C. Drag, and C. Delsart,  
 332 *Eur. Phys. J. D* **58**, 29 (2010).
- 333 [24] E. Tiesinga, P. J. Mohr, D. B. Newell, and B. N. Taylor, *The*  
 334 *2018 CODATA recommended values of the fundamental physi-*  
 335 *cal constants (web version 8.0)* (National Institute of Standards  
 336 and Technology, Gaithersburg, 2019), URL <http://physics.nist.gov/constants>.
- 337 [25] G. Cerchiari, S. Erlewein, P. Yzombard, M. Zimmermann, and  
 338 A. Kellerbauer, *J. Phys. B* **52**, 155003 (2019).
- 339 [26] J. Huba, *NRL Plasma Formulary* (Naval Research  
 340 Laboratory, Plasma Physics Division, 2018), URL  
 341 [https://www.nrl.navy.mil/ppd/sites/www.nrl.navy.mil/ppd/files/pdfs/NRL\\_FORMULARY\\_18.pdf](https://www.nrl.navy.mil/ppd/sites/www.nrl.navy.mil/ppd/files/pdfs/NRL_FORMULARY_18.pdf).
- 342 [27] L. Spitzer, *Physics of Fully Ionized Gases: Second Revised Edi-*  
 343 *tion* (Dover, 2013), ISBN 9780486449821.
- 344 [28] M. Drewsen and A. Brønner, *Phys. Rev. A* **62**, 045401 (2000).